

Supplementary Material:

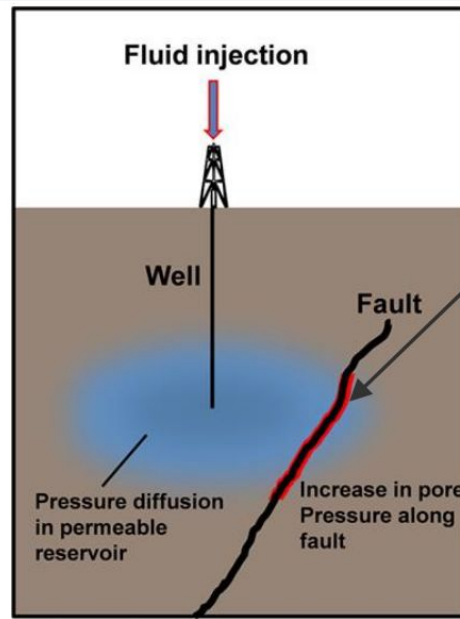
Injection Rate effects on failure of a saturated gouge- filled Fault: Dilation vs. Diffusion

Pritom Sarma¹, Einat Aharonov^{1,2}, Stanislav Parez³ & Renaud Toussaint^{4,2}

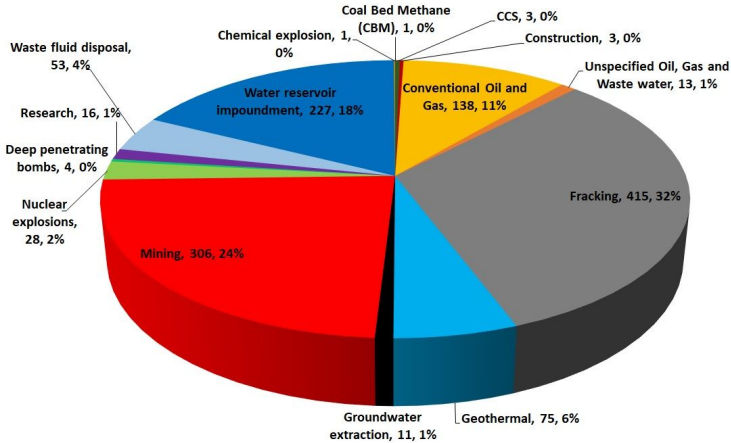
- 1) Institute of Earth Sciences, Hebrew University of Jerusalem, Israel.
- 2) PoreLab, The Njord Centre, Departments of Physics and Geosciences, University of Oslo, Norway.
- 3) Institute of Chemical Process Fundamentals, Czech Academy of Sciences, Prague, Czech Republic.
- 4) Université de Strasbourg, CNRS, Institut de Physique du Globe de Strasbourg, Strasbourg, France.

Background

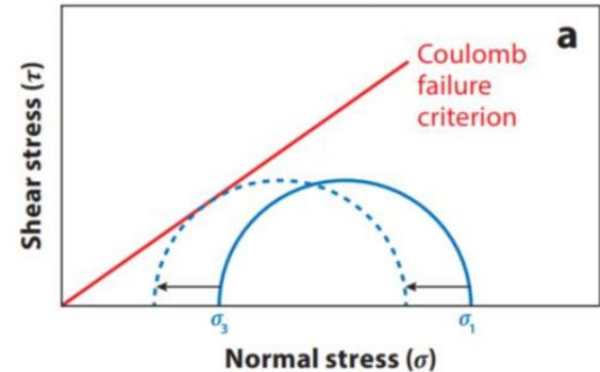
- Injection of fluids into the subsurface has been linked to fault instability, causing a) induced seismicity and b) aseismic creep.



Permeable Fault Zone



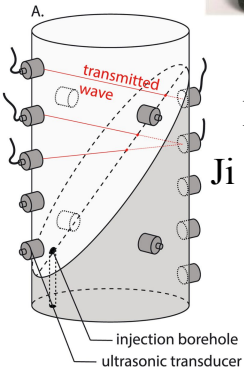
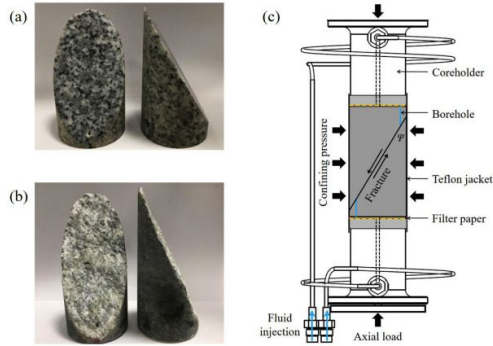
(Keranen and Weingarten, 2018)



Data Source: www.inducedearthquakes.org

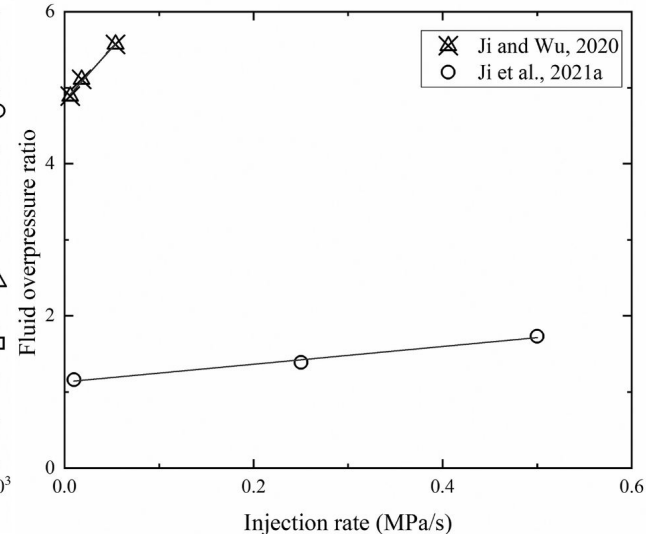
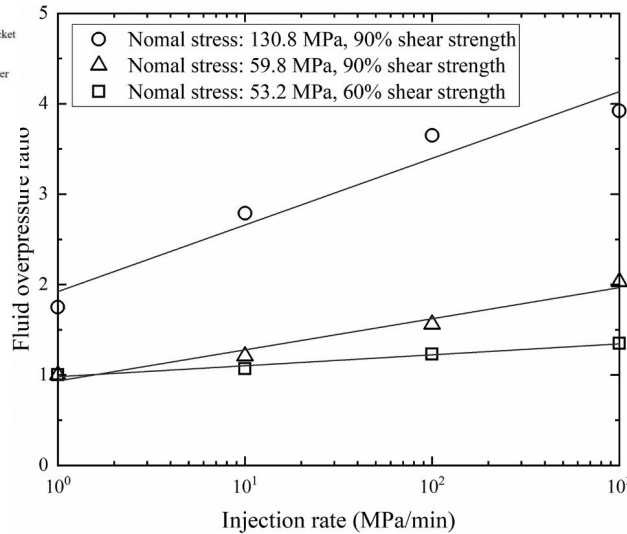
Experimental Observations: Injection Rate vs. Failure Pressure

Recent experimental studies (Passelegue et al., 2018; Ji & Wu, 2020; Ji et al., 2021) show that slower injections lead to failure at lower pressures than fast injection rates.



Passelegue et al., 2018
 Ji & Wu, 2020; Ji et al., 2021

$$\text{Fluid Overpressure Ratio} = \frac{\text{Injection Pressure at Fault Failure}}{\text{Predicted Fluid Pressure with the Mohr-Coloumb failure criterion}}$$



Formulation for the physics of pore fluid

Grains mass conservation :

$$\frac{\partial[(1-\phi)\rho_s]}{\partial t} + \nabla \cdot [(1-\phi)\rho_s u_s] = 0$$

Fluid mass conservation :

$$\frac{\partial[\phi\rho_f]}{\partial t} + \nabla \cdot [\phi\rho_f u_f] = 0$$

Darcy :

$$u_f - u_s = -\frac{k}{\mu\phi} \nabla p$$

Fluid state :

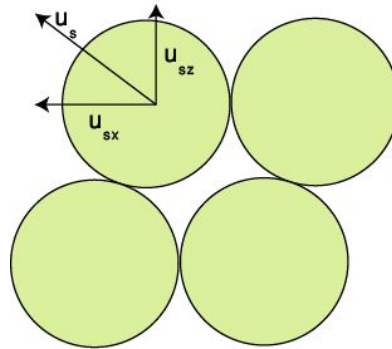
$$\rho_f = \rho_0 (1 + \beta p)$$

Fluid compressibility



Under the assumption of nearly incompressible grains, but deformable media

$$\frac{\partial p}{\partial t} = \frac{1}{\beta\phi} \nabla \cdot \left[\frac{k}{\mu} \nabla p \right] - \frac{1}{\beta\phi} \nabla \cdot u_s$$



$$\nabla \cdot u_s = \frac{\partial\Phi/\partial t}{\Phi(1-\Phi)}$$

It can be shown that this formulation is a generalization of:

Wang, 2000

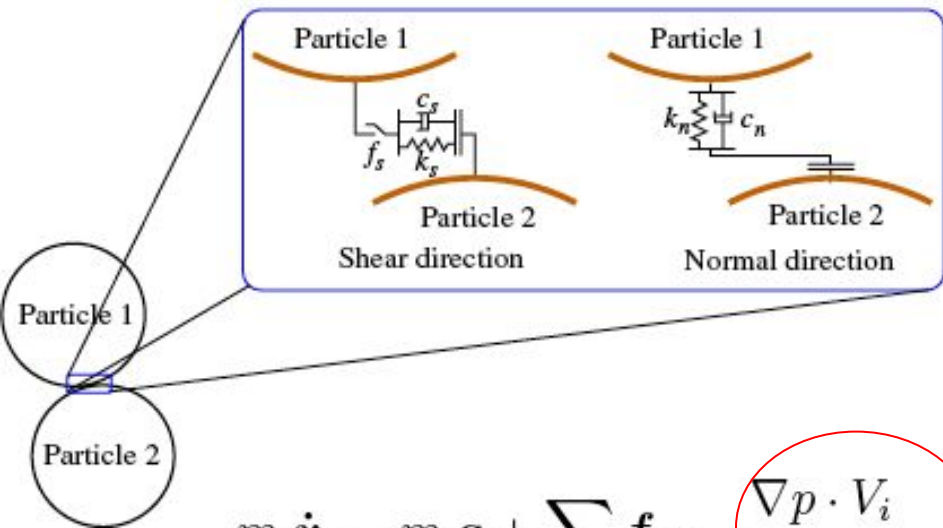
z+ Bechraich et al., 2001 (when neglecting inertia)

Walder & Nur, 1984

Snieder & van der Beukel, 2004

Samuelson et al., 2009

Adding the grains



$$m_i \dot{\mathbf{v}}_i = m_i \mathbf{g} + \sum_j \mathbf{f}_{ij} - \frac{\nabla p \cdot \mathbf{V}_i}{1 - \phi}$$

$$I_i \dot{\boldsymbol{\omega}}_i = \sum_j \mathbf{R}_{ij} \times \mathbf{f}_{ij}$$

Normal force on grain i:

$$\mathbf{f}_{ij}^n = [k_n (R_i + R_j - r_{ij}) - \gamma_n m (\dot{\mathbf{r}}_{ij} \cdot \hat{\mathbf{n}})] \hat{\mathbf{n}}$$

Elastic repulsive force
Viscous damping

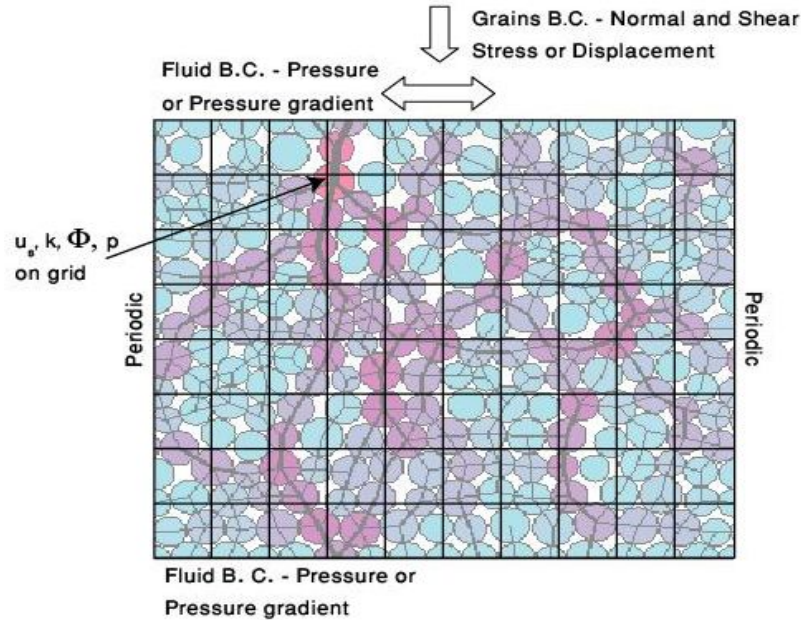
Shear force on grain i:

$$\mathbf{f}_{ij}^s = -\{\min[k_s \Delta s, \mu(\mathbf{F} \cdot \hat{\mathbf{n}})]\} \hat{\mathbf{s}}$$

Elastic shear force
Frictional resistance

Linear and angular momentum of grain i:

2-phase 2-scale model



Permeability evolution is given by 3D Carman-Kozeny relationship:

$$k = \frac{k_c(1 + 2\phi)^2}{(1-\phi)^2}$$

Solid deformation changes the fluid pressure via the divergence in solid velocity

$$\nabla \cdot \mathbf{u}_s$$

And the local geometry as expressed by the porosity, permeability

$$\phi, \mathbf{k}$$

The fluid pressure gradients ∇P act as a force affecting the solid grain motion.

End-member cases of fluid flow

- We consider a simple **pore-fluid** equation including **compaction source** and **darcian diffusion** (Goren et. al., 2010, 2011).

$$\frac{\partial P}{\partial t} - \frac{1}{\beta\Phi\eta} \nabla \cdot [k\nabla P] + \frac{1}{\beta\Phi(1-\Phi)} \frac{\partial \Phi}{\partial t} = 0.$$

DILATIVE SOURCE

- Where **P(x,t)** is the **pore pressure**, **β** is the **adiabatic fluid compressibility**, **φ** is the **porosity**, **η** is the **viscosity of the fluid** and **k** is the **permeability**.

Diffusive End Member:

- Following is the **diffusive end member**, with **initial and boundary conditions**

$$\frac{\partial P}{\partial t} - \frac{1}{\beta\Phi\eta} \nabla \cdot [k\nabla P] = 0. \quad \longleftarrow \mathbf{I}$$

IC: $P(x, 0) = 0$ & **BC:** $P(0, t) = P(L, t) = \dot{P}_0 t$

- Plugging in the solution to Eqn **I** in a Mohr Coulomb Failure criterion

$$P_{boundary} = \dot{P}_0 t = \sigma_n - \sigma_T / \mu + \frac{L^2 \dot{P}_0}{8D}$$

- $P_{boundary}$ is the injected pressure during failure, σ_n is the normal stress, σ_T is the shear stress, μ is the static friction coefficient, L is the length of the domain, D is the hydraulic diffusivity of the medium and \dot{P}_0 is the rate of injection.

Dilative End Member:

- Following is the **dilative end member**

$$\frac{1}{\beta\Phi\eta} \nabla \cdot [k\nabla P] + \frac{1}{\beta\Phi(1-\Phi)} \frac{\partial\Phi}{\partial t} = 0. \longleftarrow \mathbf{II}$$

- We restructure the source term w.r.t the **strain rate** \dot{h}/h

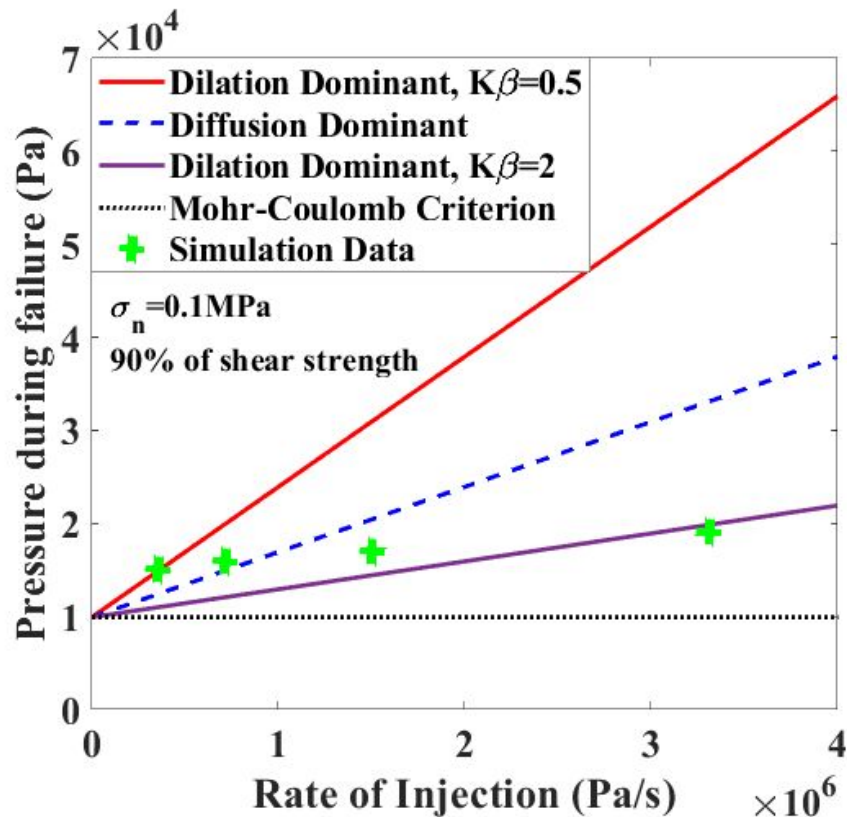
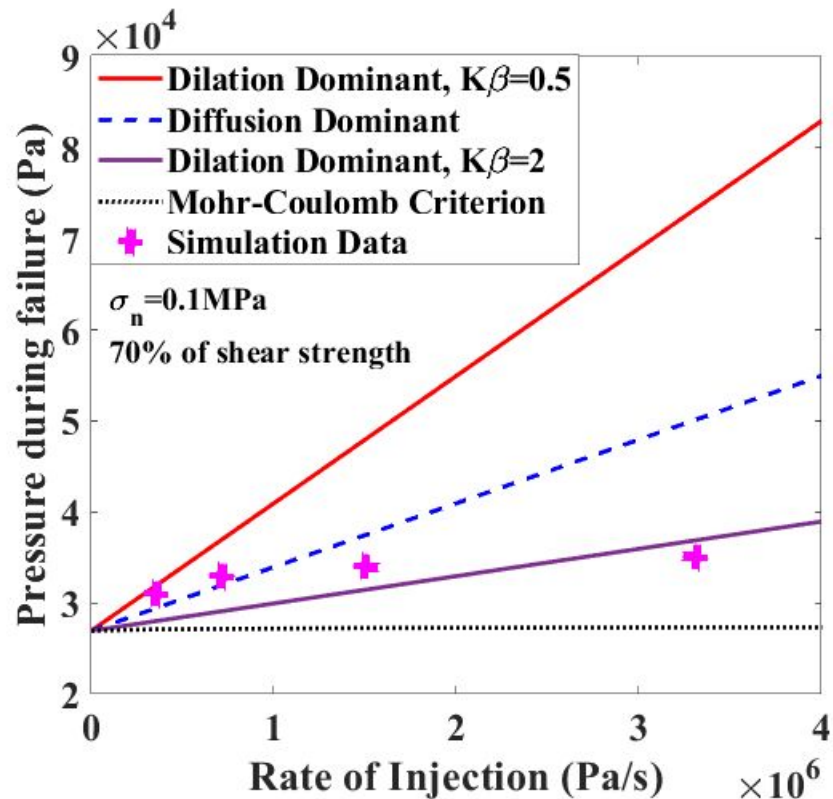
$$\frac{1}{\Phi(1-\Phi)} \frac{\partial\Phi}{\partial t} = \dot{h}/h$$

- Plugging in the solution with the same initial and boundary conditions as discussed above to Eqn **II** in a Mohr Coulomb Failure criterion

$$P_{boundary} = \dot{P}_o t_s = \sigma_n - \sigma_T/\mu + \frac{L^2}{8D} \frac{\dot{P}_o}{K\beta}$$

- **K** is the Young's modulus of the grain packing and **β** is the adiabatic fluid compressibility.

Supplementary Results



References

- Keranen, K. M., & Weingarten, M. (2018). Induced seismicity. *Annual Review of Earth and Planetary Sciences*, 46, 149-174.
- Passelègue, F. X., Brantut, N., & Mitchell, T. M. (2018). Fault reactivation by fluid injection: Controls from stress state and injection rate. *Geophysical Research Letters*, 45(23), 12-837.
- Ji, Y., Fang, Z., & Wu, W. (2021). Fluid overpressurization of rock fractures: experimental investigation and analytical modeling. *Rock Mechanics and Rock Engineering*, 54, 3039-3050.
- Ji, Y., & Wu, W. (2020). Injection-driven fracture instability in granite: mechanism and implications. *Tectonophysics*, 791, 228572.
- Ji, Y., Hofmann, H., Duan, K., & Zang, A. (2022). Laboratory experiments on fault behavior towards better understanding of injection-induced seismicity in geoenery systems. *Earth-Science Reviews*, 226, 103916.
- McNamara, S., Flekkøy, E. G., & Måløy, K. J. (2000). Grains and gas flow: Molecular dynamics with hydrodynamic interactions. *Physical review E*, 61(4), 4054.
- Goren, L., Aharonov, E., Sparks, D., & Toussaint, R. (2011). The mechanical coupling of fluid-filled granular material under shear. *Pure and Applied Geophysics*, 168, 2289-2323.
- Goren, L., Aharonov, E., Sparks, D., & Toussaint, R. (2010). Pore pressure evolution in deforming granular material: A general formulation and the infinitely stiff approximation. *Journal of Geophysical Research: Solid Earth*, 115(B9).
- Ben-Zeev, S., Aharonov, E., Toussaint, R., Parez, S., & Goren, L. (2020). Compaction front and pore fluid pressurization in horizontally shaken drained granular layers. *Physical Review Fluids*, 5(5), 054301.
- Ben-Zeev, S., Goren, L., Toussaint, R., & Aharonov, E. (2023). Drainage explains soil liquefaction beyond the earthquake near-field. *Nature Communications*, 14(1), 5791.
- Parez, S., Kozakovic, M., & Havlica, J. (2023). Pore pressure drop during dynamic rupture and conditions for dilatancy hardening. *Journal of Geophysical Research: Solid Earth*, 128(7), e2023JB026396.
- van den Ende, M., Scuderi, M. M., Cappa, F., & Ampuero, J. P. (2020). Extracting microphysical fault friction parameters from laboratory and field injection experiments. *Solid Earth*, 11(6), 2245-2256.